

ORIGINAL ARTICLE

# Capsaicin modulates *Akkermansia muciniphila* abundance by enhancing MUCIN2 levels in mice fed with high-fat diets

Ting Gong<sup>1</sup>, Yujing Zhou<sup>2#</sup>, Qin hong Shi<sup>2</sup>, Yanyan Li<sup>2</sup>, Haizhu Wang<sup>2</sup>, Min Zhang<sup>2\*</sup> and Linzheng Liao<sup>3\*</sup>

<sup>1</sup>Chongqing college of traditional chinese medicine, school of general education, Chongqing, China; <sup>2</sup>Chongqing Medical and Pharmaceutical College, College of nursing, Chongqing, China; <sup>3</sup>Chongqing University of Arts and Science, Horticultural Plant Engineering Research Center of Chongqing Universities, Chongqing, China

## Popular scientific summary

- Capsaicin enhances the secretion of colonic mucin MUC2 through TRPV1, providing ample carbon and sources for *A. muciniphila*, promotes its proliferation, and thus regulates abnormal lipid metabolism.

## Abstract

Extensive research has been conducted to investigate the impact of capsaicin (CAP) on lipid metabolism, focusing specifically on its interaction with the vanilloid subtype 1 (TRPV1) ion channel. Additionally, studies have illuminated the role of *Akkermansia muciniphila* (*A. muciniphila*), a specific strain of intestinal microbiota, in lipid metabolism. In this study, a model utilizing resiniferatoxin (RTX) was employed to deactivate TRPV1 ion channels in germ-free mice, followed by the administration of *A. muciniphila* via gavage. Following the collection of intestinal tissues for a comprehensive analysis, employing histopathology, qPCR, and ELISA techniques, our findings revealed a significant upregulation of MUC2 and MUC3 expression induced by CAP. This upregulation resulted in the thickening of the colonic mucus layers. Notably, this effect was absent when TRPV1 was selectively inhibited. Moreover, there was no discernible impact on goblet cells. The findings strongly indicate that CAP influences the system by activating the TRPV1 ion channel, thereby enhancing the expression of mucin MUC2 and promoting an augmentation in the thickness of the mucous layer. This activation, in turn, supplies *A. muciniphila* with an ample source of carbon and nitrogen. This insight potentially clarify the underlying mechanism through which CAP facilitates the increase in *A. muciniphila* abundance.

Keywords: *capsaicin*; *TRPV1*; *Akkermansia muciniphila*; *MUC2*

To access the supplementary material, please visit the article landing page

Received: 4 September 2023; Revised: 26 October 2023; Accepted: 8 December 2023; Published: 17 April 2024

Numerous scientific investigations have extensively explored the robust correlation between intestinal microorganisms and metabolic irregularities triggered by a high-fat diet. Intestinal microorganisms have recently emerged as a novel focal point for modulating abnormal lipid metabolism (1). Specifically, *Akkermansia muciniphila* (*A. muciniphila*), a Gram-negative anaerobic bacterium categorized in the *Akkermansia* genus of the *Verrucomicrobia* phylum,

has gained recognition (2). This bacterium is widely acknowledged for its role in mucin degradation and is heralded as a next-generation probiotic capable of regulating glucose metabolism, mitigating low-grade inflammation, restraining fat accumulation, and ameliorating lipid metabolism disorders (1, 3–5).

Capsaicin (CAP), a naturally occurring compound found in select foods, has been implicated in the regulation of abnormal lipid metabolism. Numerous studies have

#Co-First author: Yujing Zhou (271766235@qq.com), Chongqing Medical and Pharmaceutical College, Chongqing, 400715, P.R. China

delved into the mechanisms through which CAP influences abnormal lipid metabolism. The transient receptor potential vanilloid subtype 1 (TRPV1) ion channel, acting as a sensor for CAP, has been reported to participate in the regulation of lipid metabolism (6). However, recent research has revealed that CAP-induced alterations in intestinal microorganisms result in increased abundance of *A. muciniphila* and other bacterial strains, along with elevated levels of short-chain fatty acids (7–9). Nevertheless, the precise mechanism underlying CAP's promotion of increased *A. muciniphila* abundance remains elusive.

*A. muciniphila* is an anaerobic chemo-organotroph that relies exclusively on mucin as its source of nitrogen, carbon, and energy (10–12). Consequently, our study sought to elucidate the mechanisms driving the heightened abundance of *A. muciniphila* induced by CAP in high-fat diet-induced obese mice through an evaluation of mucin levels.

## Materials and methods

### Materials

CAP ( $\geq 95\%$ ) was acquired from Henan bis-biotech Co., Ltd., China. *A. muciniphila* ATCC BAA-835 was procured from the American Type Culture Collection.

### Animals and treatments

A total of 50 male specific germ-free Kunming mice, aged 6–8 weeks and weighing 25–40 g, were obtained from the Laboratory Animal Center of Army Medical University in China. The Institutional Animal Care and Use Committee of Army Medical University (AMUWEC20226157) approved the experimental protocols. Germ-free KM Tac mice were bred and housed in plastic gnotobiotic isolators at Army Medical University. The mice were individually housed in cages maintained at a temperature of  $25 \pm 1^\circ\text{C}$ , with a relative humidity of 40–70% and subjected to a 12-h light/12-h dark cycle. The experiment spanned 4 weeks. Prior to the commencement of the experiment, the mice were provided unrestricted access to water and a standard diet for 1 week. Subsequently, the mice were randomly divided into four groups ( $n = 10$ ): the high-fat diet group (HF), the high-fat diet group supplemented with 0.01% CAP (HC), the high-fat diet + 0.01% CAP + resiniferatoxin (RTX) (200  $\mu\text{g}/\text{kg}$  body weight of the animal) (HCR), the high-fat diet + 0.01% CAP +  $2 \times 10^8$  CFU *A. muciniphila* (HCA), and the high-fat diet + 0.01% CAP + RTX (200  $\mu\text{g}/\text{kg}$  body weight of the animal) +  $2 \times 10^8$  CFU *A. muciniphila* (HCRA). CAP was integrated into the mice's chow, with the dosage selection based on relevant studies (8, 13). The composition of the diets for the experimental groups is detailed in Supplementary Table S1. The high-cholesterol feed included a 1% cholesterol supplement in accordance with the US Standard AIN-93 feed formula (14).

### Sample collection

Throughout the trial, daily monitoring was conducted to assess animal mortality. The mice's body weight and food consumption were documented on a weekly basis. At the end of the 4-week period, the mice were euthanized to facilitate the collection of blood samples, along with samples from the colon, cecum, small intestine, and their respective contents. Blood samples were collected through eyeball extraction. The remaining samples were promptly placed in germ-free containers and flash-frozen in liquid nitrogen for 30 sec. Subsequently, they were stored at  $-80^\circ\text{C}$  until further analysis. All procedures were executed meticulously under aseptic conditions.

### Chemodenervation and confirmation tests

Successful ablation of TRPV1+ neurons in the HR and HCR group animals was achieved through a single intraperitoneal injection of the maximum tolerable dose of RTX (200  $\mu\text{g}/\text{kg}$  body weight). The confirmation of effective ablation was based on the absence of observed physiological responses after 24 h, following a method adapted from prior literature with minor adjustments (15). To validate the ablation, two tests were conducted: the hot plate test and the eye wipe test. In the hot plate test, the surface temperature was meticulously maintained at  $60 \pm 5^\circ\text{C}$ , and the number of jumps or paw licks within a 15-sec interval was documented. Each animal underwent the test three times, with a 5-min interval between repetitions. The eye wipe test entailed the administration of a 0.02% (w/v) CAP solution, and the number of eye wipes within a 30-sec period was recorded. Replicates were independently taken from each eye of the animal.

### Mucin2 analysis

The levels of MUC2 in the colon were measured using an enzyme-linked immunoassay (ELISA) kit (Sinobestio, Shanghai).

### Histopathologic analysis

After fixation in 10% buffered formalin, the colon tissue samples underwent a series of steps. They were dehydrated using various ethanol concentrations, followed by clearing in xylene. Subsequently, the samples were embedded in paraffin blocks and sliced into approximately 5  $\mu\text{m}$  thick sections. These sections were then subjected to staining with Periodic Acid-Schiff (PAS) to facilitate histopathological assessment and visualization of the thickness of the colonic mucus layer. To visualize the goblet cells in the colon tissue, a combination of Alcian Blue (AB)-PAS stain and nuclear fast red (Sigma-Aldrich) staining techniques was employed. Microphotographs of all the histological slides were captured using a light imaging microscope (BX40F4, NIKON, Tokyo, Japan). Finally, the mean thickness was calculated using an image analysis program.

### RNA isolation and quantitative real-time polymerase chain reaction

Total RNA was extracted from the colon tissue of the mice using the Ribopure RNA extraction kit (Invitrogen, USA), following the manufacturer's instructions. For cDNA synthesis, 1  $\mu$ g of total RNA was employed with a RT-PCR kit (Invitrogen, Rockville, MD) and the SuperScript III First-Strand Synthesis System. The resulting cDNA derived from the total RNA was analyzed using a real-time quantitative PCR system (CFX96 Touch™ Real-Time PCR Detection System, Bio-Rad, USA). The specific primers used for the genes of interest in this study are listed in Supplementary Table S2. The relative gene expression values were determined using the  $\Delta\Delta$ Ct method ( $\Delta\Delta$ Ct =  $\Delta\Delta$ Ct treated -  $\Delta\Delta$ Ct untreated control), and the equation  $y = 2^{-\Delta\Delta$ Ct was applied.  $\beta$ -Actin served as the reference gene, and mRNA levels in different experimental groups were compared to those of the control group, which were normalized to 1 (16).

### Statistical analysis

The data were presented as mean  $\pm$  standard deviation ( $n = 8$ ). Statistical analysis was conducted using Origin

8.5 and SPSS version 20.0. One-way analysis of variance (ANOVA) was utilized, followed by Duncan's multiple-range test to evaluate differences among the groups. A significance level of  $P < 0.05$  was considered statistically significant.

## Results

### Behavioral validation of selective ablation of TRPV1

In mice, the administration of RTX led to the complete elimination of physiological responses to noxious heat and CAP. During the hot plate test, neither jumping nor paw licking behaviors were observed in the HCR and HCRA groups (Fig. 1A and B), indicating a complete insensitivity to temperatures ( $60 \pm 5^\circ\text{C}$ ). These findings validate the systemic ablation of TRPV1 receptors in the treated animals. To evaluate the response to CAP-induced pain, a 0.02% (w/v) CAP solution was employed in the eye wipe test. Similarly, no response was observed in the HCR and HCRA groups, while the control group exhibited frequent eye wiping (Fig. 1C). These results are consistent with previous studies on TRPV1 denervation using RTX.

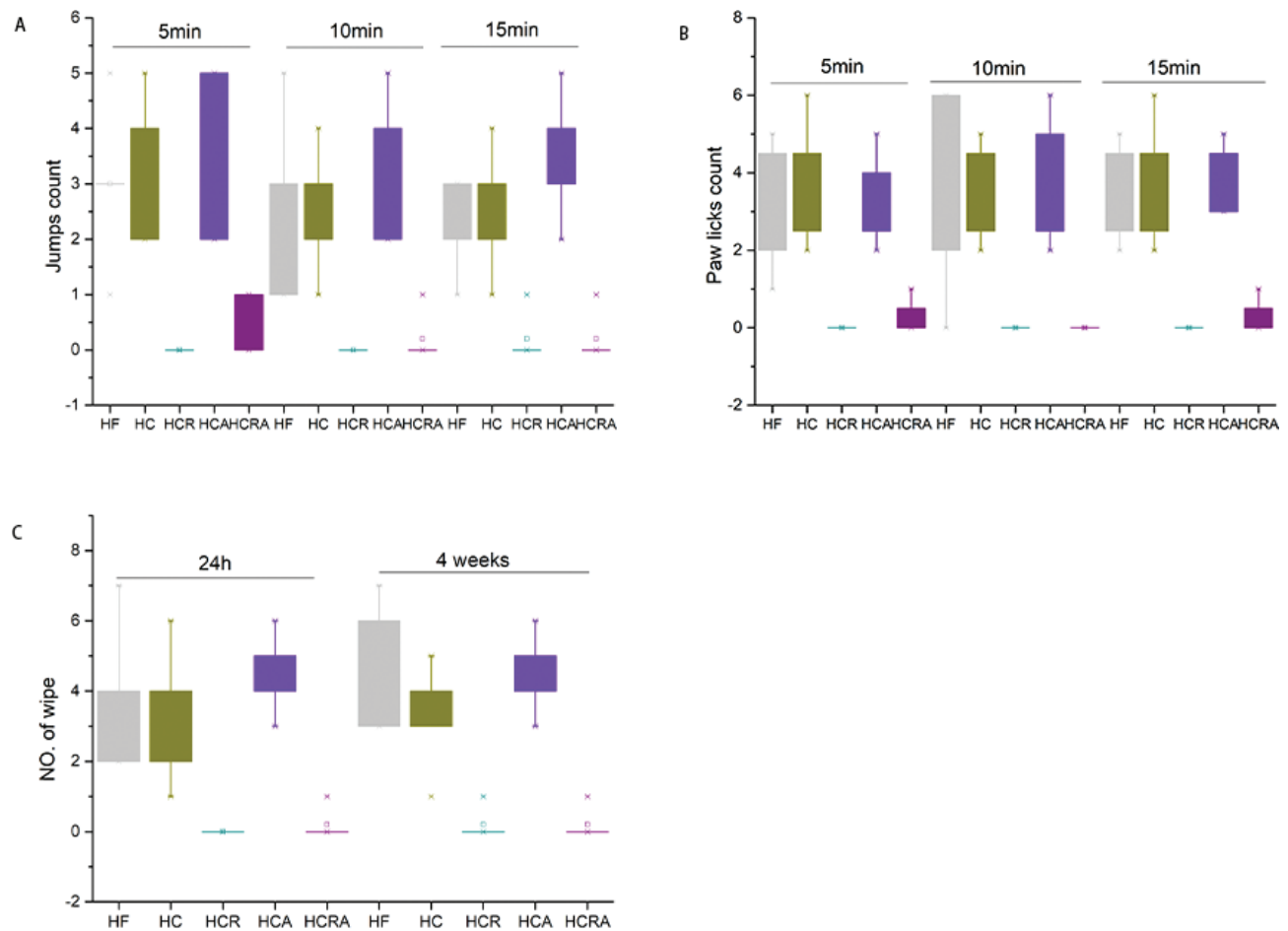


**Fig. 1.** (A–C) Behavioral pain assays for validating TRPV1 denervation in RTX-treated mice. (A–B) Hot plate test; (C) Eye wipe test.

Furthermore, these consistent outcomes persisted in the eye wipe test even after a 4-week period (Fig. 1C), confirming the absence of significant recovery of TRPV1+ neurons.

#### Effect of CAP on weight gain and food intake of germ-free mice

The body weight of the HC and HCR groups decreased by 53.7 and 48.9%, respectively, in comparison to the HF group (Fig. 2A). Two weeks later, the HC group displayed notably reduced food intake in comparison to the HCR group. Moreover, the HCRA group exhibited increased food intake compared to the HCA group.

#### Effect of CAP on the number of colonic goblet cells of germ-free mice in different treatment groups

Figure 3 presents the histopathological analysis of excised tissue from various experimental groups. In the HF, HC, and HCR groups, the intestinal structure appeared normal, with no reduction in the number of crypts in the mucosal layer. The epithelial cells displayed a well-organized and tightly packed arrangement, and goblet cells were abundant. Similarly, in the HCA group, the intestinal structure was largely normal, with no decrease in the number of crypts in the mucosal layer. The epithelial cells exhibited a well-arranged and tightly packed pattern, without any noticeable degeneration or shedding. Furthermore, there was a significant presence of goblet cells within the crypts. In the HCRA group, the intestinal structure also appeared normal, with no reduction in the number of crypts in the mucosal layer. The epithelial cells were neatly arranged and tightly packed, showing no signs of denaturation, and

a substantial number of goblet cells were observed (Fig. 3A). The quantification of goblet cells in the visual field was performed using Image-Pro Plus 6.0 software. Statistical analysis revealed that the number of goblet cells in the HCA group did not exhibit significant changes, but it was slightly higher compared to the other groups (Fig. 3B).

#### Effect of CAP on mucous layer of germ-free mice in different treatment groups

Figure 4A illustrates the visualization of mucous layer thickness in the inner colon wall using PAS staining. In Fig. 4B, it is evident that the inclusion of CAP led to a notable increase in mucous layer thickness in the HC group by 8.96  $\mu\text{m}$ . In contrast, following the selective ablation of TRPV1 by RTX, the mucous layer thickness in the HCR group significantly decreased to 5.15  $\mu\text{m}$ . The mucous layer thickness in the HCA, HCR, and HCRA groups was notably lower compared to the HC group, with no significant differences observed among the HCA, HCR, and HCRA groups.

#### Effect of CAP on colonic mucin content of germ-free mice in different treatment groups

According to the results depicted in Fig. 5, the mucin content in the HC group displayed a substantial increase of 63.3% when compared to the HF group, and a 51.3% increase in comparison to the HCR group. Furthermore, there was a significant elevation of 33.9% in mucin content in the HC group when contrasted with the HCA group. Although the HCRA group exhibited a marginal increase in mucin content in comparison to the HCR group, this difference did not achieve statistical significance.

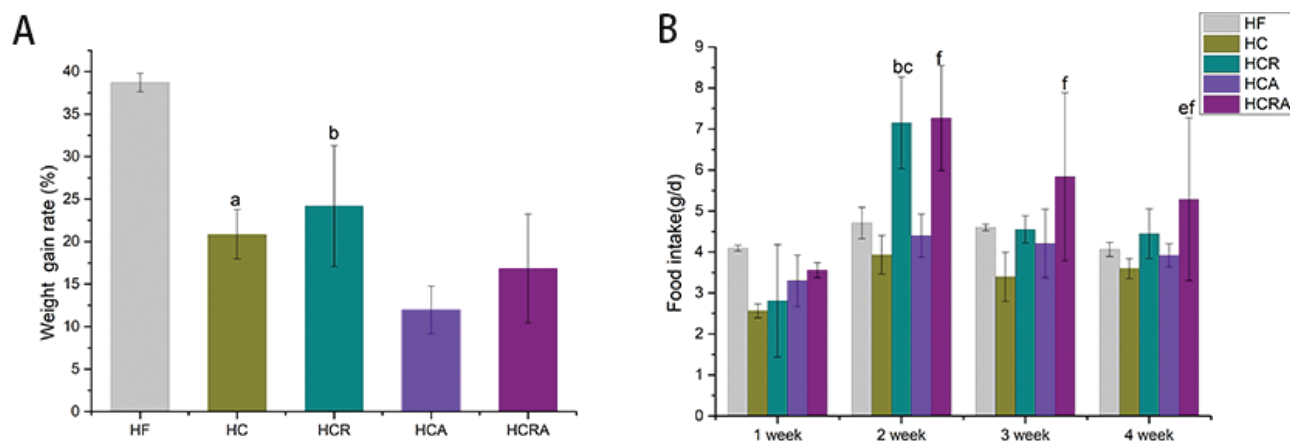


**Fig. 2.** Effects of CAP on body weight (A) and feed intake (B) of germ-free mice in different treatment groups. Note: Values are expressed as mean  $\pm$  standard deviation ( $n = 10$ ). 'a' denotes a significant difference between the HF and HC groups. 'b' denotes a significant difference between the HF and HCR groups. 'c' denotes a significant difference between the HC and HCR groups. 'd' denotes a significant difference between the HC and HCA groups. 'e' denotes a significant difference between the HCR and HCRA groups. 'f' denotes a significant difference between the HCA and HCRA groups (Dunnett test after one-way ANOVA,  $P < 0.05$ ).

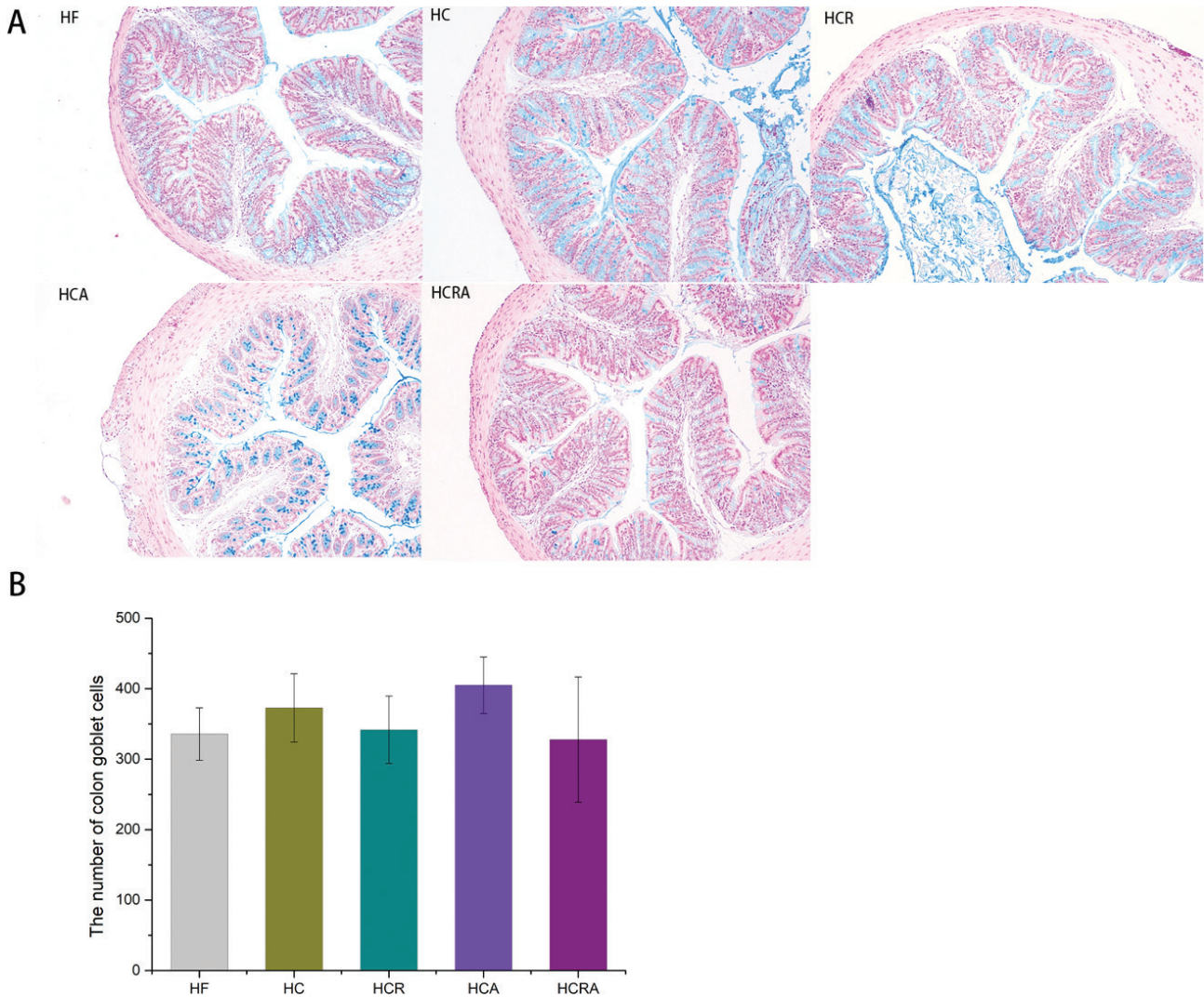


**Fig. 3.** (A) AB-PAS staining (100 $\times$ ) of goblet cells in colon tissue. (B) Quantification of goblet cells in colonic tissue. Note: Values are expressed as mean  $\pm$  standard deviation ( $n = 10$ ) (Dunnett test after one-way ANOVA,  $P < 0.05$ ).

#### Effect of CAP on genes related to colonic mucin secretion of germ-free mice in different treatment groups

Figure 6 illustrates the impact of CAP on genes associated with mucin secretion in the colons of germ-free mice across various treatment groups. The expression of *Klf4* in the colon did not reveal any significant differences among the groups. However, *TRPV1* expression in the HC group exhibited a substantial increase, with a 99.1% elevation compared to the HF group, a 280.7% increase compared to the HCR group, and a 107.7% increase compared to the HCRA group. Furthermore, in comparison to the HF group, *Muc2* expression in the HC group displayed a significant increase of 339.1%, while the HCR group demonstrated a notable increase of 280.4%. Additionally, *MUC3* expression in the HC group was significantly higher than that in the HF, HCR, and HCA groups.

#### Discussion

*A. muciniphila* is a bacterium found in the human intestinal tract, first isolated from stool samples in 2004. Its distinctive capability to facilitate the degradation of mucin within the gut positions it as a crucial organism residing at the interface between the intestinal lumen and host cells. Despite its relatively recent discovery, *A. muciniphila* stands as the sole cultured representative of the Verrucomicrobia phylum, readily detectable in phylogenetic and metagenomic analyses, thereby distinguishing it as one of the prominent phyla in the human gut (17). Reduced levels of *A. muciniphila* have been consistently noted in individuals with inflammatory bowel disease, notably ulcerative colitis, and those with metabolic disorders, implying its potential anti-inflammatory properties (18). Furthermore, *A. muciniphila* has exhibited beneficial effects across various pathological conditions,

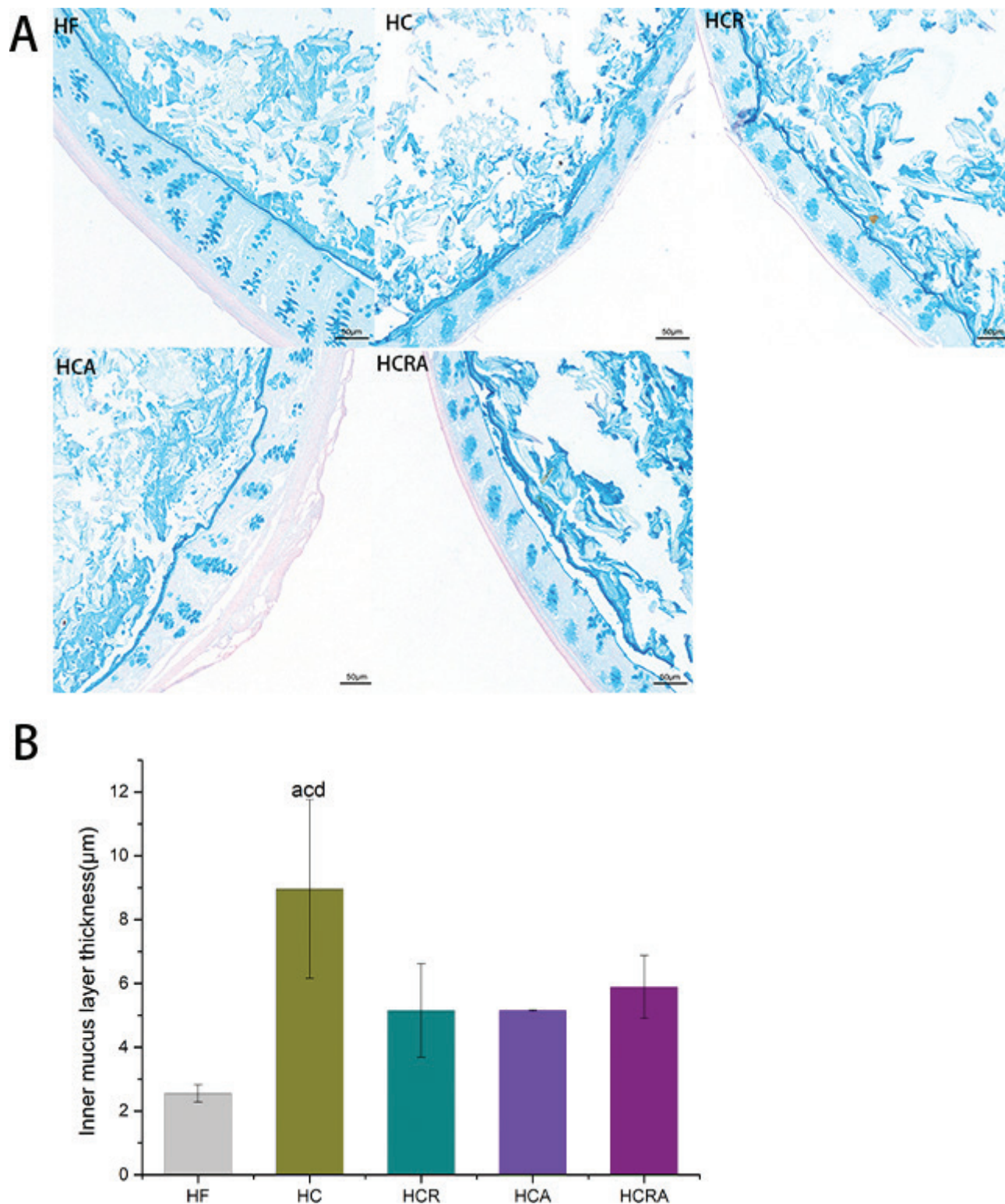


**Fig. 4.** (A) PAS staining of the mucous layer. (B) Analysis of the thickness of the mucous layer. Note: Values are expressed as mean  $\pm$  standard deviation ( $n = 10$ ). 'a' denotes a significant difference between the HF and HC groups. 'b' denotes a significant difference between the HF and HCR groups. 'c' denotes a significant difference between the HC and HCR groups. 'd' denotes a significant difference between the HC and HCA groups. 'e' denotes a significant difference between the HCR and HCRA groups (Dunnett test after one-way ANOVA,  $P < 0.05$ ).

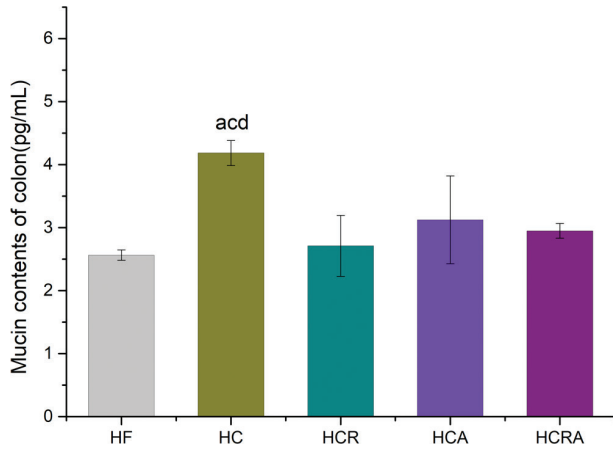


**Fig. 5.** Effects of CAP on colonic mucin content of germ-free mice in different treatment groups. Note: Values are expressed as mean  $\pm$  standard deviation ( $n = 10$ ). 'a' denotes a significant difference between the HF and HC groups. 'b' denotes a significant difference between the HF and HCR groups. 'c' denotes a significant difference between the HC and HCR groups. 'd' denotes a significant difference between the HC and HCA groups. 'e' denotes a significant difference between the HCR and HCRA groups (Dunnett test after one-way ANOVA,  $P < 0.05$ ).

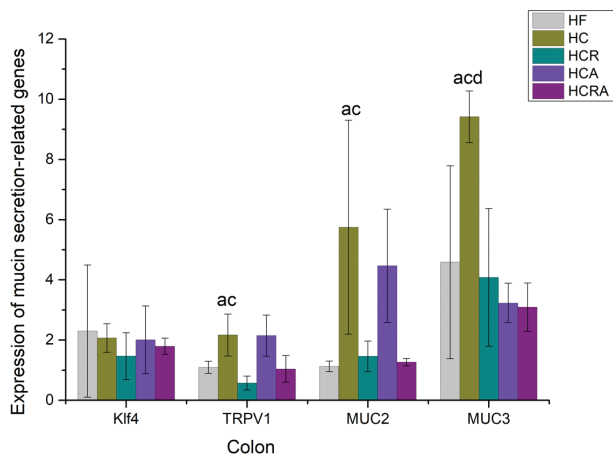


**Fig. 6.** Effect of CAP on genes related to colonic mucin secretion of germ-free mice in different treatment groups. Note: Values are expressed as mean  $\pm$  standard deviation ( $n = 10$ ). 'a' denotes a significant difference between the HF and HC groups. 'b' denotes a significant difference between the HF and HCR groups. 'c' denotes a significant difference between the HC and HCR groups. 'd' denotes a significant difference between the HC and HCA groups. 'e' denotes a significant difference between the HCR and HCRA groups (Dunnett test after one-way ANOVA,  $P < 0.05$ ).

encompassing lipid reduction, inflammation mitigation, delayed aging, enhanced immunity, and the regulation of the nervous system (19).

Multiple studies have documented the ability of CAP to elevate the abundance of *A. muciniphila* in mice (7, 8). It has been reported that CAP's impact on

*A. muciniphila* abundance is mediated by the TRPV1 channels (20). Consequently, we selectively incapacitated TRPV1 ion channels via intraperitoneal injection of RTX. Subsequently, we confirmed the successful modeling of the HCR and HCRA groups by observing their unresponsiveness to heat and pain stimuli during the hot plate experiment at  $60 \pm 5^\circ\text{C}$  and the CAP-induced ocular discomfort experiment. In contrast, the relevant control group exhibited conspicuous jumping and eye rubbing behaviors in response to both stimuli. Hence, our modeling results align with the findings reported by Kumar et al. (15). In terms of body weight, we observed a notable decrease in the body weight of mice in both the HC and HCR groups. However, the feed intake of the HCR and HCRA groups exhibited a significant increase compared to that of the HC group. This heightened feed consumption may be attributed to the stimulated desensitization of CAP in mice following the selective ablation of TRPV1 by RTX.

The colon epithelium primarily consists of closely connected cells, including columnar, cup-shaped, and enteric endocrine cells, representing differentiated epithelial lineages (21). Goblet cells play a crucial role in mucin secretion, forming the physical barrier of the colonic mucosa (22). Therefore, we conducted a histopathological analysis to evaluate the number of colonic goblet cells in germ-free mice subjected to selective TRPV1 ablation. The analysis revealed no significant differences in the number of goblet cells among the treatment groups. This finding suggests that CAP and selective ablation of TRPV1 have no impact on the goblet cell count, consistent with the results reported by Shen Wei et al. (20).

The mucous layer functions as a critical defense mechanism, safeguarding the intestinal lining against microorganisms and other luminal compounds. In the colon, it assumes an additional role as it harbors a distinct microbial community known as the mucus-associated microbiome (23). This microbial community has evolved alongside the host over an extended period, establishing a mutually beneficial relationship (24). The mucus layer contributes to various host functions, including facilitating efficient mucin turnover and stimulating goblet cells through toll-receptor mediation to promote mucus production (25). Continuous mucus production is essential for maintaining the integrity of the intestinal barrier and can inhibit the growth of pathogenic bacteria by generating antimicrobial compounds and promoting the growth of beneficial bacteria (26). Moreover, the mucus-associated microbiota confers 'colonization resistance' by occupying the pathogenic niche with symbiotic species and producing metabolites that interact with both the microbes and the host, significantly influencing the development of the host immune system (27).

*A. muciniphila* produces several mucolytic enzymes that degrade mucus, serving as its primary carbon and nitrogen source (3). Consequently, it is considered a key member of the mucus-associated flora (28). In our analysis of the mucous layer in mice from different treatment groups, we observed a significant difference in the thickness of the mucous layer between the HC and HCR groups, suggesting that CAP may promote mucous layer secretion. Conversely, the mucous layer in the HCA group was significantly thinner than that in the HC group, possibly due to *A. muciniphila* utilizing the mucous layer as a nitrogen source. Although the difference between the HCRA and HCR groups did not reach statistical significance, there was a slight increase in mucous layer thickness in the HCRA group compared to the HCR group, which could be attributed to the inherent ability of *A. muciniphila* to stimulate mucous layer growth (29).

The intestinal mucus layer primarily consists of Mucin 2 (MUC2), a highly glycosylated gel produced by goblet cells (30). Alongside epithelial cells, MUC2 forms a protective barrier against harmful substances. It constitutes a major component of the colonic mucosal layer, known for its role in inhibiting intestinal inflammation and preventing the formation and progression of intestinal tumors (31–33). *A. muciniphila*, a probiotic bacterium, is recognized for its ability to degrade human intestinal mucin (15). It possesses more than 300 genes that potentially participate in mucin degradation (34). A recent study identified a secreted protein from *A. muciniphila*, named Amuc\_1434, capable of breaking down MUC2 (3). Consequently, we assessed the levels of MUC2 in the colon. Our findings indicated that the MUC2 levels in the HC group were significantly higher than those in the HF group, suggesting that CAP may promote the increase of MUC2, corroborating the results reported by Shen Wei et al. (20). When CAP was administered to mice with selective TRPV1 ablation, we observed a notable decrease in MUC2 levels compared to the HC group, implying that the inactivation of TRPV1 ion channels might hinder MUC2 secretion. Nevertheless, both the HCA and HCRA groups exhibited a decrease in MUC2 levels compared to the HC group, likely attributable to the depletion of MUC2 induced by the colonization of *A. muciniphila*.

*KLF4*, a transcription factor containing zinc finger motifs, regulates the formation and differentiation of colonic goblet cells during mouse development (35). We found no significant difference in *KLF4* expression in the colon among the various treatment groups, indicating that CAP did not exert a significant influence on goblet cell differentiation. Our results demonstrated that CAP can stimulate the expression of *MUC2* and *MUC3* genes in the colon. Furthermore, the stimulatory effect of CAP

on *MUC2* and *MUC3* expression substantially diminished after TRPV1 elimination using RTX, suggesting that TRPV1 may play a pivotal role in CAP-induced expression of *MUC2* and *MUC3* in the colon. These findings align with our prior observations regarding mucin content. In summary, these results suggest that CAP enhances the secretion of colonic mucin MUC2 through TRPV1, providing ample carbon and nitrogen sources for *A. muciniphila* and thereby promoting its proliferation.

## Conclusions

The current study presents robust evidence that CAP can augment mucous layer thickness and elevate the expression of mucin MUC2 through TRPV1 ion channel activation. This activation, in turn, affords *A. muciniphila* an abundant supply of carbon and nitrogen, shedding light on the mechanism underlying CAP's promotion of increased *A. muciniphila* abundance. Moreover, our findings reveal a slight decrease in body weight in germ-free mice subsequent to *A. muciniphila* administration, aligning with prior research suggesting an inverse relationship between *A. muciniphila* and weight gain (36).

## Declaration of competing interest

All authors declare that they have no conflict of interest.

## Subsection ethics statement

All procedures followed were in accordance with the ethical standards of the responsible committee on human experimentation Institutional Animal Care and Use Committee of Southwest University.

## Acknowledgments

This research was supported by the Natural Science Foundation of Chongqing qing (ctsc2020jycy-msxmX0627) and City Management College (2023KYQD04) and Scientific and Technological Research Program of Chongqing Municipal Education Commission (KJQN202303312, KJQN202202819).

## Conflict of interest and funding

The authors have not received any funding or benefits from industry or elsewhere to conduct this study.

## References

- Zhou Q, Zhang Y, Wang X, Yang R, Zhu X, Zhang Y, et al. Gut bacteria Akkermansia associated with reduced risk of obesity: evidence from the American Gut Project. *Nutr Metabol* 2020; 17(1): 90. doi: 10.1186/s12986-020-00516-1
- Kosciow K, Deppenmeier U. Characterization of a phospholipid-regulated beta-galactosidase from Akkermansia muciniphila involved in mucin degradation. *Microbiologyopen* 2019; 8(8): e796. doi: 10.1002/mbo3.796



3. Meng X, Wang W, Lan T, Yang W, Yu D, Fang X, et al. A Purified aspartic protease from Akkermansia Muciniphila plays an important role in degrading Muc2. *Int J Mol Sci* 2020; 21(1): 3122. doi: 10.3390/ijms21010072
4. Hussain A, Yadav MK, Bose S, Wang J-H, Lim D, Song Y-K, et al. Daesihotang is an effective herbal formulation in attenuation of obesity in mice through alteration of gene expression and modulation of intestinal microbiota. *PLoS One* 2016; 11(11): e0165483. doi: 10.1371/journal.pone.0165483
5. Rinaldi E, Consonni A, Cordiglieri C, Sacco G, Crasa C, Fontana A, et al. Therapeutic effect of Bifidobacterium administration on experimental autoimmune myasthenia gravis in Lewis rats. *Front Immunol* 2019; 10: 2949. doi: 10.3389/fimmu.2019.02949
6. Yang F, Zheng J. Understand spiciness: mechanism of TRPV1 channel activation by capsaicin. *Protein Cell* 2017; 8(3): 169–77. doi: 10.1007/s13238-016-0353-7
7. Wang Y, Tang C, Tang Y, Yin H, Liu X. Capsaicin has an anti-obesity effect through alterations in gut microbiota populations and short-chain fatty acid concentrations. *Food Nutr Res* 2020; 64: 3525. doi: 10.29219/fnr.v64.3525
8. Shen W, Shen M, Zhao X, Zhu H, Yang Y, Lu S, et al. Anti-obesity effect of capsaicin in mice fed with high-fat diet is associated with an increase in population of the gut bacterium Akkermansia muciniphila. *Front Microbiol* 2017; 8: 1–10. doi: 10.3389/fmicb.2017.00272
9. Gong T, Wang H, Liu S, Zhang M, Xie Y, Liu X. Capsaicin regulates lipid metabolism through modulation of bile acid/gut microbiota metabolism in high-fat-fed SD rats. *Food Nutr Res* 2022; 66: 8289. doi: 10.29219/fnr.v66.8289
10. Rooijers K, Kolmeder C, Juste C, Dore J, de Been M, Boeren S, et al. An iterative workflow for mining the human intestinal metaproteome. *Bmc Genom*. 2011; 12: 6. doi: 10.1186/1471-2164-12-6
11. Liou AP, Paziuk M, Luevano J-M, Jr., Machinini S, Turnbaugh PJ, Kaplan LM. Conserved shifts in the gut microbiota due to gastric bypass reduce host weight and adiposity. *Sci Transl Med* 2013; 5(178): 41. doi: 10.1126/scitranslmed.3005687
12. Brodmann T, Endo A, Gueimonde M, Vinderola G, Kneifel W, de Vos WM, et al. Safety of novel microbes for human consumption: practical examples of assessment in the European Union. *Front Microbiol* 2017; 8: 1725. doi: 10.3389/fmicb.2017.01725
13. Zhang L, Fang G, Zheng L, Chen Z, Liu X. Hypocholesterolemic effect of capsaicinoids in rats fed diets with or without cholesterol. *J Agric Food Chem* 2013; 61(18): 4287–93. doi: 10.1021/jf304471t
14. Afrose S, Hossain MS, Maki T, Tsujii H. Karaya root saponin exerts a hypocholesterolemic response in rats fed a high-cholesterol diet. *Nutr Res*. 2009; 29(5): 350–4. doi: 10.1016/j.nutres.2009.05.008
15. Kumar V, Mahajan N, Khare P, Kondepudi KK, Bishnoi M. Role of TRPV1 in colonic mucin production and gut microbiota profile. *Eur J Pharmacol* 2020; 888: 173567. doi: 10.1016/j.ejphar.2020.173567
16. Limei B, Yuanpei Z, Jun Z, Fuguang L, Lu M, Huang H, et al. The effect of cholesterol-lowering probiotics on bile acid metabolism of non-alcoholic fatty liver disease and mechanism. *Chinese J Microbiol Immunol* 2016; 36(02): 110–6.
17. Derrien M, Belzer C, de Vos WM. Akkermansia muciniphila and its role in regulating host functions. *Microb Pathogen* 2017; 106: 171–81. doi: 10.1016/j.micpath.2016.02.005
18. Macchione IG, Lopetuso LR, Ianiro G, Napoli M, Gibiino G, Rizzatti G, et al. Akkermansia muciniphila: key player in metabolic and gastrointestinal disorders. *Eur Rev Med Pharmacol Sci* 2019; 23(18): 8075–83.
19. Ma W-Y, Feng S-X, Chen N-H. Advances of Akkermansia muciniphila in regulating host functions. *Zhongguo Zhong Yao Za Zhi* 2021; 46(11): 2760–5.
20. Gong T, Zhou YJ, Zhang L, Wang HZ, Zhang M. Capsaicin combined with dietary fiber prevents high-fat diet associated aberrant lipid metabolism by improving the structure of intestinal flora [J]. *Food Science & Nutrition* 2023; 11(1): 114–25.
21. Tomas J, Reygnier J, Mayeur C, Ducroc R, Bouet S, Bridonneau C, et al. Early colonizing *Escherichia coli* elicits remodeling of rat colonic epithelium shifting toward a new homeostatic state. *ISME J* 2015; 9(1): 46–58. doi: 10.1038/ismej.2014.111
22. Li X-G, Chen M-X, Zhao S-Q, Wang X-Q. Intestinal models for personalized medicine: from conventional models to microfluidic primary intestine-on-a-chip. *Stem Cell Rev Rep* 2021; 18(6): 2137–51. doi:10.1007/s12015-021-10205-y
23. Johansson MEV, Larsson JMH, Hansson GC. The two mucus layers of colon are organized by the MUC2 mucin, whereas the outer layer is a legislator of host-microbial interactions. *Proc Natl Acad Sci U S A* 2011; 108: 4659–65. doi: 10.1073/pnas.1006451107
24. Neish AS. Microbes in gastrointestinal health and disease. *Gastroenterology* 2009; 136(1): 65–80. doi: 10.1053/j.gastro.2008.10.080
25. Birchenough GMH, Nystrom EEL, Johansson MEV, Hansson GC. Innate immunity A sentinel goblet cell guards the colonic crypt by triggering Nlrp6-dependent Muc2 secretion. *Science* 2016; 352(6293): 1535–42. doi: 10.1126/science.aaf7419
26. McGuckin MA, Linden SK, Sutton P, Florin TH. Mucin dynamics and enteric pathogens. *Nat Rev Microbiol* 2011; 9(4): 265–78. doi: 10.1038/nrmicro2538
27. Sorbara MT, Pamer EG. Interbacterial mechanisms of colonization resistance and the strategies pathogens use to overcome them (vol 12, pg 1, 2019). *Mucosal Immunol* 2019; 12(3): 840. doi: 10.1038/s41385-019-0151-7
28. Shin J, Noh J-R, Chang D-H, Kim Y-N, Kim MH, Lee ES, et al. Elucidation of Akkermansia muciniphila probiotic traits driven by mucin depletion. *Front Microbiol* 2019; 10: 1137. doi: 10.3389/fmicb.2019.01137
29. van der Lugt B, van Beek AA, Aalvink S, Meijer B, Sovran B, Vermeij WP, et al. Akkermansia muciniphila ameliorates the age-related decline in colonic mucus thickness and attenuates immune activation in accelerated aging Ercc1(-/-) mice. *Immunity Ageing* 2019; 16: 6. doi: 10.1186/s12979-019-0145-z
30. Owen CD, Tailford LE, Monaco S, Suligoj T, Vaux L, Lallement R, et al. Unravelling the specificity and mechanism of sialic acid recognition by the gut symbiont Ruminococcus gnavus. *Nat Commun* 2017; 8: 2196. doi: 10.1038/s41467-017-02109-8
31. Singh SP, Chand HS, Banerjee S, Agarwal H, Raizada V, Roy S, et al. Acetylcholinesterase inhibitor pyridostigmine bromide attenuates gut pathology and bacterial dysbiosis in a murine model of ulcerative colitis. *Digestive Dis Sci* 2020; 65(1): 141–9. doi: 10.1007/s10620-019-05838-6
32. Okada T, Kanda T, Ueda N, Ikebuchi Y, Hashiguchi K, Nakao K, et al. IL-8 and LYPD8 expression levels are associated with the inflammatory response in the colon of patients with ulcerative colitis. *Biomed Rep* 2020; 12(4): 193–8. doi: 10.3892/br.2020.1280
33. Wibowo AA, Pardjianto B, Sumitro SB, Kania N, Handono K. Decreased expression of MUC2 due to a decrease in the expression of lectins and apoptotic defects in colitis patients. *Biochem Biophys Rep* 2019; 19: 100655. doi: 10.1016/j.bbrep.2019.100655

34. van Passel MWJ, Kant R, Zoetendal EG, Plugge CM, Derrien M, Malfatti SA, et al. The genome of *Akkermansia muciniphila*, a dedicated intestinal mucin degrader, and its use in exploring intestinal metagenomes. *PLoS One* 2011; 6(3): e16876. doi: 10.1371/journal.pone.0016876
35. Qin S, Zou Y, Zhang C-L. Cross-talk between KLF4 and STAT3 regulates axon regeneration. *Nat Commun* 2013; 4: 2633. doi: 10.1038/ncomms3633
36. Ross MC, Muzny DM, McCormick JB, Gibbs RA, Fisher-Hoch SP, Petrosino JF. 16S gut community of the Cameron County Hispanic Cohort. *Microbiome* 2015; 3: 7. doi: 10.1186/s40168-015-0072-y

---

**\*Min Zhang**

Chongqing Medical and Pharmaceutical College,  
Chongqing, 400715, P.R. China  
Email: 893511732@qq.com

**\*Linzhen Liao**

Chongqing University of Arts and Science  
No. 319 Honghe Road,  
Yongchuan District,  
Chongqing 404020, China  
Email: 20000008@cqwu.edu.cn